PHYSICAL REVIEW C VOLUME 24, NUMBER 4 OCTOBER 1981

Energy dependence of the ^{208}Pb(^{4}He,t) and (^{4}He,^{3}He) reaction from 10 to 20 MeV/nucleon

R. Perry, A. Nadasen, D.L. Hendrie,* P.G. Roos, and N.S. Chant
Department of Physics and Astronomy, University of Maryland, College Park, Maryland 20742
(Received 25 March 1981)

Alpha particle elastic scattering from ^{208}Pb and the ^{208}Pb(^{4}He,t)^{209}Bi and ^{208}Pb(^{4}He,^{3}He)^{209}Pb reactions have been measured at 39.8, 61.5, and 81.4 MeV. Distorted-wave Born approximation calculations, including finite range effects, provide spectroscopic factors for the lowest levels which are generally energy independent to within 15%. This result is in contrast to published ^{16}O+^{208}Pb single nucleon transfer studies which show a factor of approximately four variation in the spectroscopic factor over the same MeV/nucleon energy range.

[NUCLEAR REACTIONS ^{208}Pb(α,α), ($\alpha,^3$He), (α,t), E_α=39.8, 61.5, 81.4 MeV, measured $\sigma(\theta)$, enriched target; optical model analysis, DWBA analysis, deduced spectroscopic factors.]

I. INTRODUCTION

For nuclear structure information using transfer reactions, the extracted spectroscopic factors should be independent of the type and energy of projectile used. Thus, any energy dependence observed in transfer reactions should be predicted by theory, such as the distorted wave Born approximation (DWBA).

However, in the analysis of the ^{208}Pb(^{16}O,^{15}N)^{209}Bi reaction[1] it has been observed that the energy dependence of the cross section is much less than that predicted by DWBA. In spite of good fits to the shapes of the angular distributions, spectroscopic factors were found to decrease by approximately a factor of 4 in doubling the bombarding energy. The authors suggest that this effect may arise from (i) strong polarization of the shell-model orbital of the transferred nucleon by the heavy ion projectile core, (ii) coupled-channel effects among low-lying collective states, and/or (iii) the use of an inappropriate potential for the transferred nucleon. It is not clear if any or all of these suggestions can eliminate the discrepancy between experiment and the DWBA theory. However, Khanna and Pieper[2] have recently reanalyzed these data. By refitting the elastic scattering data with a potential containing an energy dependent surface imaginary term, they are able to remove most of the energy dependence from the DWBA analysis. It would certainly enhance our understanding of heavy-ion interactions to be able to confirm that the parametrization of the optical model potential is, in fact, the origin of the discrepancy, or that polarization effects or coupled-channel effects are important.

To help elucidate this problem we have chosen to study the same transfer reactions with a light-ion projectile in the same energy per nucleon range. Transfer reactions with light-ion projectiles have been successfully employed for many years in extracting nuclear structure information. We have measured the single proton and neutron transfer reactions using alpha particle projectiles of equivalent velocity, viz., 40, 60, and 80 MeV. Concurrent data were taken for the elastic scattering in order to obtain consistent entrance channel potentials.

A brief description of the experiment is given in Sec. II, and the experimental results are presented in Sec. III. Results of optical model calculations and comparison with DWBA predictions are discussed in Sec. IV. Section V summarizes the results.

II. EXPERIMENT

The experiment was carried out using incident beams from the University of Maryland Isochronous Cyclotron. Beams of 39.8, 61.5, and 81.4 MeV alpha particles were momentum analyzed

($\Delta p/p \leq 0.03\%$) and focused at the center of a 1.5 m diameter precision scattering chamber. The target used was 1 mg cm^{-2} isotopically pure (99%) ^{208}Pb evaporated onto a 10 μg cm^{-2} ^{12}C backing.

The outgoing particles were detected by two telescopes with a fixed separation angle of approximately 6° mounted on a remotely controlled arm. Each consisted of a Si ΔE detector (200 μm at 40 MeV and 500 μm at the higher energies) followed by a 5 mm Si(Li) E detector. The smaller angle telescope subtended 0.22 msr and the larger angle telescope, 0.36 msr. A 4 mm Si(Li) detector subtending a solid angle of 0.2 msr mounted on a second arm served as a monitor.

Coincidences between the ΔE and E detectors were used to gate the linear energy signals. The linear ΔE and E signals as well as those from the monitor detector were sent to a 4096 channel analog-to-digital converter (ADC) interfaced to an IBM 360/44 computer. Particle identification and energy addition were performed by computer software and ^{4}He, ^{3}He, and ^{3}H energy spectra were generated. These data were written on magnetic tape for each run. The energy resolution was better than 100 keV for the 40 and 60 MeV runs, but was only 150 keV at 80 MeV. This resolution was sufficient to resolve the first four single particle states in ^{209}Bi and the first three in ^{209}Pb. A pulser system triggered by the current integrator was fed into each preamplifier in order to correct for the dead time of the system.

The relative normalization for the two telescopes was measured to better than 2% by obtaining data at a number of overlapping angles. The zero angle of the beam was measured to $\pm 0.05°$ by measuring elastic scattering on both sides of the beam. The absolute normalization of the data was tested using forward angle elastic scattering and is believed to be better than 7%. Furthermore, since an identical setup was used at all energies, the relative normalization between data at different energies is better than this.

The present 40 MeV (α,t) data agree very well within the 7% limit on absolute normalization with previous 42 MeV ^{208}Pb(α,t) data.[3] On the other hand, our 61.5 MeV $(\alpha,^3\text{He})$ data are at variance with the 58 MeV data of Tickle and Gray[4] for angles less than 30°. However, in the present experiment, both elastic scattering and (α,t) data were obtained concurrently with the $(\alpha,^3\text{He})$ data. Considering the similarity of the (α,t) and $(\alpha,^3\text{He})$ data, our agreement with previous 40 MeV (α,t) data, and the fact that the ratio of the elastic scattering cross section to the Rutherford scattering cross section reaches unity at forward angles, we believe the present data to be correct.

III. EXPERIMENTAL RESULTS

Elastic scattering data at the three energies were obtained up to about 65°. These are shown in Fig. 1. The statistical errors in the data range from about 1–2% at the smallest angles to about 10% at the largest angles. The data extend over 5–7 orders of magnitude in this angular range and show a strong contribution from Coulomb scattering.

The (α,t) data for the lowest 4 states in ^{209}Bi are plotted in Figs. 2–4, along with DWBA calculations discussed in Sec. IV. In spite of a change of five units in the angular momentum, at each energy the angular dependence of the states is very similar, reflecting the large momentum mismatch. Also, the data at 60 and 80 MeV are quite similar,

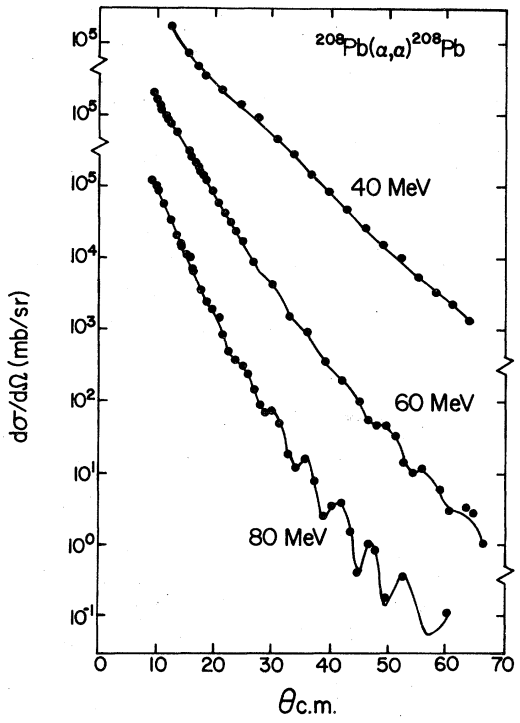

FIG. 1. Differential cross sections for elastic scattering of ^{4}He from ^{208}Pb at three energies. The solid curves are the result of optical model fits.

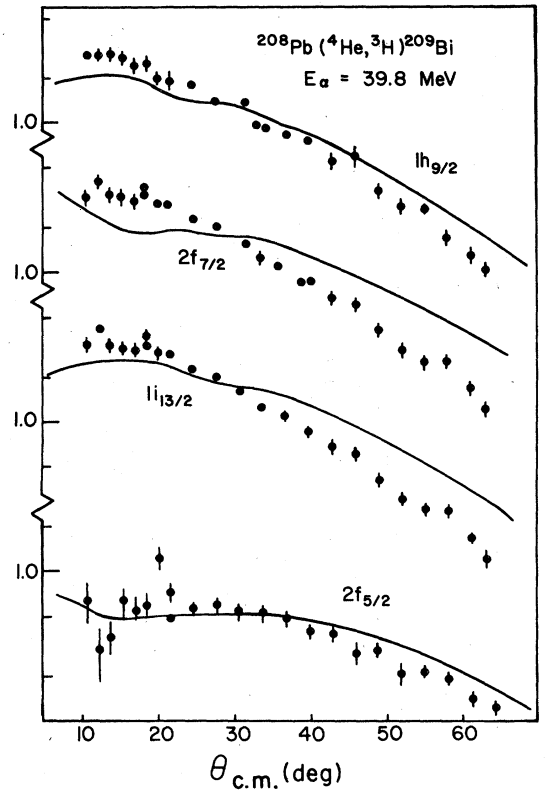

FIG. 2. (^{4}He,^{3}H) differential cross sections at 39.8 MeV for the four lowest levels in ^{209}Bi. The angular distributions are labeled by the single particle state in ^{209}Bi. The curves are finite range DWBA calculations normalized to the data.

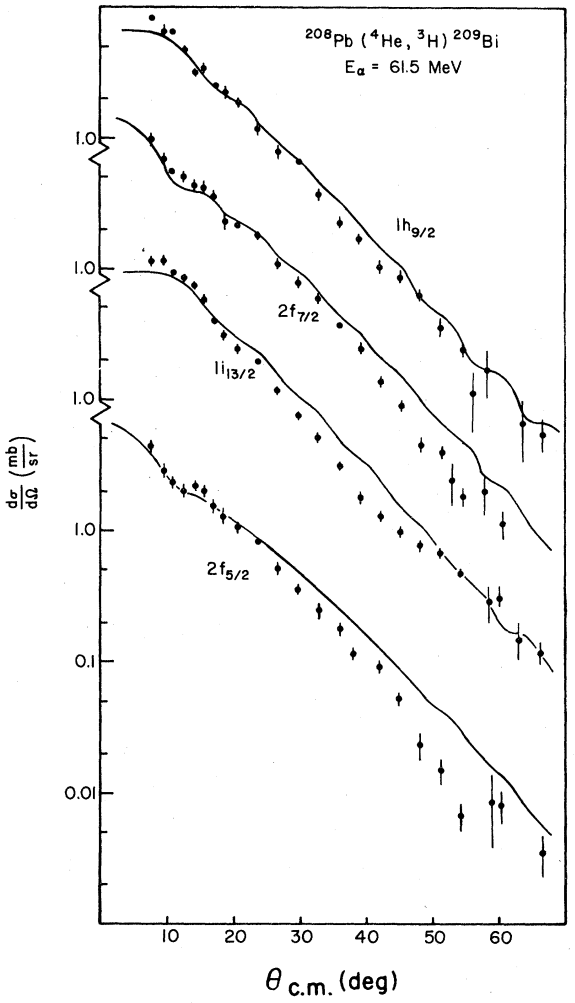

FIG. 3. (^{4}He,^{3}H) differential cross sections at 61.5 MeV (see caption of Fig. 2).

whereas the 40 MeV data fall off more slowly with angle. The (α,^{3}He) data for the three lowest states of ^{209}Pb are presented in Figs. 6 and 7. They are similar in structure to the (α,t) data.

IV. THEORETICAL ANALYSIS

A. Optical model analysis

The elastic scattering data were analyzed with an optical model potential of the form

$$U(r)=U_{\text{Coul}}(r)-Vf_0(r)-iW_Vf_w(r),$$

where $U_{\text{Coul}}(r)$ is the Coulomb potential due to a uniform sphere of charge of radius $r_CA^{1/3}$ and

$$f_i(r)=\left[1+\exp\left[\frac{r-r_iA^{1/3}}{a_i}\right]\right]^{-1}.$$

The Coulomb radius parameter r_C was fixed at 1.25 fm, and searches were made on all six parameters of the central nuclear potential. Because of the limited angular range of the data, two families of potentials provide equally good fits, with volume integrals per nucleon pair around 300 MeV fm^3 (shallow) and 400 MeV fm^3 (deep). After initial searches average geometrical parameters were deduced and the data refitted in order to obtain systematic potentials for the DWBA analysis. This procedure produced no deterioration in the fits for the deep potentials, but we were unable to find a fixed geometry consistent with the 40 MeV data for the shallow potentials. The resultant parameters are shown in Table I. The energy dependence of both sets of potentials are consistent with previ-

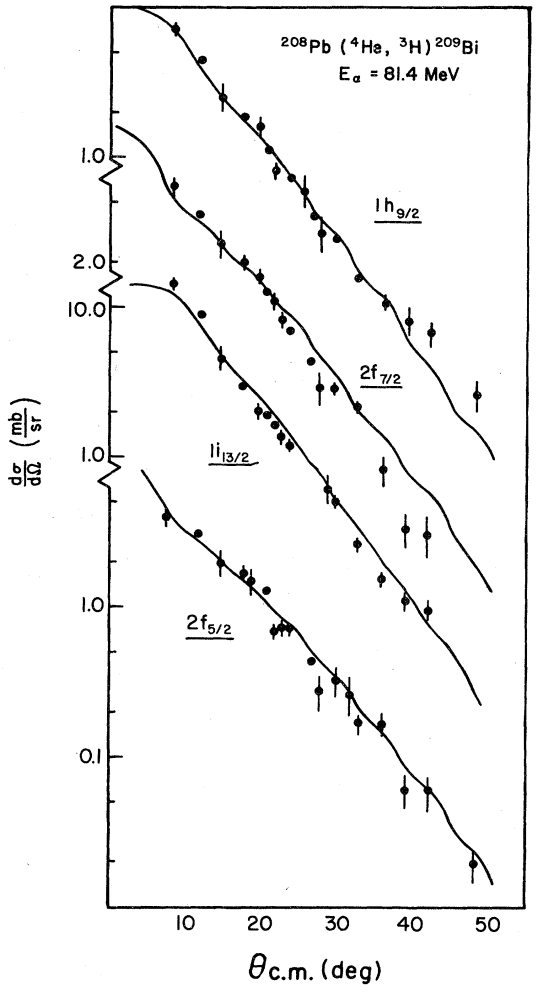

FIG. 4. (^{4}He,^{3}H) differential cross sections at 81.4 MeV (see caption of Fig. 2).

ous analyses of alpha elastic scattering data.[5,6] We obtained an average energy dependence for the real volume integral of

$$J_R(E)/4A = J_R(0)/4A - [1.3\pm0.3]\cdot E \text{ MeV fm}^3.$$

For the imaginary volume integral we obtained

$$J_W(E)/4A = J_W(0)/4A + (2.5\pm0.5)E \text{ MeV fm}^3$$

from 40–60 MeV, but there seems to be no significant change between 60 and 80 MeV, in agreement with the results of Singh *et al.*[5]

B. ^{208}Pb$(\alpha,t)^{209}$Bi DWBA calculations

The DWBA calculations were carried out using the exact finite range code MARY written by Chant.[7] In the notation of Ref. 7, the range function chosen was

$$V(s)Y_{00}(\hat{s}) = \langle \phi_b \mid V_{bx} \mid \phi_a \rangle,$$

where the wave functions ϕ_i describing the ^{3}H (^{3}He) and ^{4}He particles were taken as 1s oscillator functions with size parameters chosen to fit radii obtained from the electron scattering. The ejectile-nucleon interaction V_{bx} was taken as a sum of singlet and triplet Gaussian nucleon-nucleon potentials which fit low energy nucleon-nucleon scattering.[8]

Calculations were also carried out in the zero-range approximation to examine the effects of finite range at these energies. We find that the *ZR* and *FR* calculations produce nearly identical shapes, differing only in magnitude. Furthermore, the ratio of cross sections (*FR*/*ZR*) is state and energy independent to within about 10% as long as a consistent set of optical potentials is used. If the zero range calculations are normalized in the usual way to the volume integral D_0 of our chosen range function, our choice of optical model parameters lead to a *FR*/*ZR* ratio of roughly two. This result is in agreement with estimates of the ratio of the parameters D^2 and $D_0{}^2$ discussed by Friedman and others.[9] It is consistent with the assumption that the reaction is rather strongly surface localized.

The optical model parameters used for generating distorted waves in the entrance channel were the fixed geometry "deep family" potentials derived from the present elastic scattering analysis. Although the shallow potentials provide very similar results, the deep potentials were adopted because of their consistency.

For the triton exit channel we have the difficulty that no triton elastic scattering data exist at the higher energies required for this analysis. The global analysis by Becchetti and Greenlees[10] of ^{3}He and t elastic scattering incorporating a complex symmetry potential strongly overestimates the strength of the imaginary symmetry potential, at least at higher energies. The results of Ref. 10 lead to a total imaginary potential which goes to zero near 70 MeV. As a result, for the two higher energy (α,t) data sets, the triton potential is very shallow leading to calculated angular distributions which oscillate, in disagreement with the experimental data. Thus, these potentials are inappropri-

TABLE I. Optical model potential parameters.[a]

	T_α (MeV)	V_0	r_0	a_0	W_0	r_0'	a'	J_R	χ^2/N
				^{4}He parameters					
	40	181.1	1.32	0.62	15.13	1.35	0.85	463	2.1
Deep	61.5	167.3	1.32	0.62	26.11	1.35	0.85	428	1.0
	81.4	158.4	1.32	0.62	30.02	1.35	0.85	405	4.1
	40	98.6	1.435	0.606	11.93	1.629	0.212	319	1.5
Shallow	61.5	112.6	1.342	0.600	22.15	1.437	0.725	304	0.9
	81.5	106.1	1.329	0.682	20.76	1.460	0.762	280	1.5

^{3}He(t) exit channel parameters

T_α (MeV)	V_0	r_0	a_0	W_0	r_0'	a'
40	131.7	1.182	0.857	17.2	1.551	0.769
61.5	128.5	1.182	0.857	17.2	1.551	0.769
81.4	125.4	1.182	0.857	17.2	1.551	0.769

Bound-state parameters[b]

Type	r_0	a_0	V_{so}	r_{so}	a_{so}
proton	1.28	0.76	6.0	1.09	0.6
neutron	1.25	0.63	6.0	1.10	0.5

[a]Potential of the form $U(r)=-V_0 f(x)-iW_0 f(x')+V_{\text{Coulomb}}$, where

$$f_i(x)=\left[1+\exp\left[\frac{r-r_i A^{1/3}}{a_i}\right]\right]^{-1}$$

and V_{Coulomb} is the Coulomb potential of a uniform sphere of charge of radius $1.25\,A^{1/3}$.
[b]Strength adjusted to reproduce empirical separation energies. The spin-orbit potential is of the form

$$-V_{so}\left[\frac{\hbar}{m_\pi c}\right]^2 \vec{l}\cdot\vec{\sigma}\frac{1}{r}\frac{d}{dr}f(x_{so}),$$

where $f(x_{so})$ is the Woods-Saxon form with radius and diffuseness parameters r_{so} and a_{so}, respectively.

ate for the analysis in the energy range spanned by the present experiment. We believe that for these strongly absorbed particles the imaginary part of the triton potential at the higher energies is more likely comparable to that of the ^{3}He potential. Therefore, the triton potential was obtained from an analysis of ^{3}He+^{208}Pb elastic scattering at 130 MeV.[11] The strengths of the potentials were adjusted according to the energy dependence of ^{3}He elastic scattering extracted in Ref. 12. These potentials are also listed in Table I. Although the energy dependence of the strengths were included, it is worth noting that the present (α,t) calculations are extremely insensitive to variations in the magnitude of the strength introduced by this energy dependence.

Since it is our intention to make a comparison with the heavy ion transfer results of Ref. 1, we adopted the bound state Woods-Saxon potential used therein (see Table I). The results of these calculations normalized to the experimental data are shown in Figs. 2–4. The fits to the data at the two higher energies, are quite satisfactory. However, at 40 MeV the calculation underpredicts the cross section at forward angles, or more correctly predicts too little slope for the angular dependence of the cross section. Closer inspection of the higher energy data suggests a similar but less pronounced discrepancy.

In order to examine this discrepancy in shape we

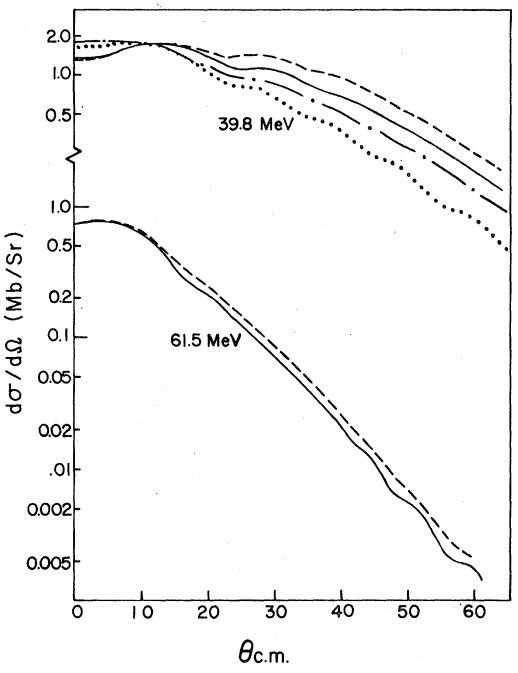

FIG. 5. DWBA calculations for the ^{208}Pb(^{4}He,^{3}H)^{209}Bi (9/2-ground state) reaction at 39.8 and 61.5 MeV using various optical model potentials (——, ^{3}H and ^{4}He potentials in Table I; — — —, ^{3}H from Ref. 13, ^{4}He from Table I; —·—,^{3}H and ^{4}He from Ref. 14; · · · ,^{3}H and ^{4}He from Ref. 3).

have carried out a series of calculations using various optical model parameters. The use of the shallow ^{4}He potentials presented in Table I produces very little difference in shape compared with the present calculations. Similarly, variations in the strengths of the real and imaginary potentials in both the entrance and exit channels by 10% produce insignificant changes. This variation is probably more consistent with the differences expected due to the isospin dependence. Calculations were then carried out with a ^{3}He potential obtained by Parkinson *et al.*[13] from an analysis of ^{3}He elastic scattering from ^{208}Pb at 47.5 MeV. These calculations for 40 and 60 MeV compared to our present calculations are shown in Fig. 5. Since their slope is less, it is clear that the agreement with the data will be worse.

We have also tried the ^{4}He and triton potentials used by Flynn *et al.*[14] in their analysis of 17 MeV ($\vec{t}$,α) studies on lead istopes. Their calculations produce moderately good agreement with their data. The calculations for 40 MeV [nearly the same c.m. energy as the (t,α) studies] are also shown in Fig. 5. They provide a somewhat improved fit to the 40 MeV data, but a significant discrepancy in slope still remains. Considering the fact that we are striving for consistency in the analysis, and that the normalization of the Flynn calculation is nearly the same as our original calculation, we see no reason to replace the original calculations with these results.

Finally, we have carried out calculations with the ^{4}He and triton potentials used by Lilley and Stein[3] to analyze their 42 MeV ^{208}Pb(α,t) data. These calculations produce good agreement with their data as well as our 40 MeV data. The calculation for the ground state is shown in Fig. 5. However, these potentials are much deeper (V_α=200 MeV, V_t=299 MeV) than is consistent with present day knowledge of these complex light ion potentials. Furthermore, they produce significant change in the normalization. Again from the standpoint of consistency, and the fact that these potentials are inconsistent with higher energy elastic scattering results, we have excluded them from consideration.

Based on these various studies we have chosen to use the results for the original potentials. The extracted spectroscopic factors for the normalization shown in the figures are presented in Table II. It should be noted that the calculations have no normalization beyond that of the spectroscopic factor, and the absolute C^2S values are nearly those expected for pure single particle states. These results indicate that the finite range calculation with the chosen range function adequately reproduces the magnitude of the cross section. In this connection it is worth noting that other studies suggest that oscillator wave functions are not adequate for treating finite range effects in transfer reactions in contrast to our own results. In general, these studies obtain V_{bx} by operating appropriately with a kinetic energy operator,[7] whereas we obtain V_{bx} directly from nucleon-nucleon scattering. Thus, it would appear that it is the inability of the oscillator functions to generate an accurate interaction which is the major deficiency of the earlier studies.

It is clear that we do not observe the large variation noted for the (^{16}O,^{15}N) reaction.[1] Our values of C^2S are in better agreement with those extracted for the higher energy heavy ion reactions.

C. ^{208}Pb(α,^{3}He)^{209}Pb DWBA calculations

For the neutron stripping reaction, we obtained data at bombarding energies of 60 and 80 MeV.

TABLE II. Spectroscopic factors for proton and neutron transfer.

Reaction	Energy levels (MeV)	J^π	Orbital	C^2S Incident ^{4}He energy 39.8 MeV	61.5 MeV	81.4 MeV
^{208}Pb(α,t)^{209}Bi	0.00	$\frac{9}{2}^-$	$1h_{9/2}$	0.82	0.90	0.82
	0.89	$\frac{7}{2}^-$	$2f_{7/2}$	0.82	0.85	0.78
	1.61	$\frac{13}{2}^+$	$1i_{13/2}$	0.82	0.88	0.78
	2.84	$\frac{5}{2}^-$	$2f_{5/2}$	0.93	0.68	0.78
^{208}Pb(α,^{3}He)^{209}Pb	0.00	$\frac{9}{2}^+$	$2g_{9/2}$		0.86	0.75
	0.78	$\frac{11}{2}^+$	$1i_{11/2}$		0.69	0.58
	1.42	$\frac{15}{2}^-$	$1j_{15/2}$		0.98	0.90

As expected, the Coulomb barrier was too large to obtain reasonable data at 40 MeV. DWBA calculations were carried out using the same potentials as for the (α,t) reaction. The results, normalized to the data are shown in Figs. 6 and 7, and the extracted spectroscopic factors are given in Table II.

Agreement between the data and the calculations of the angular distributions is again reasonably good, with some indication of difficulties at forward angles at 60 MeV.

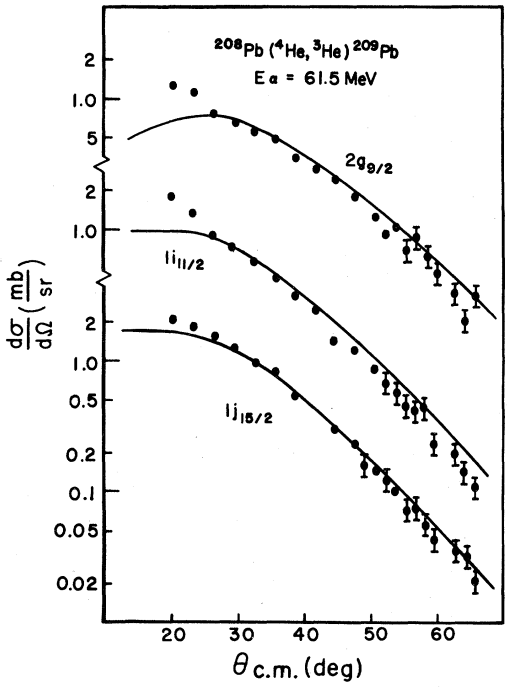

FIG. 6. (^{4}He,^{3}He) differential cross sections at 61.5 MeV (see caption of Fig. 2).

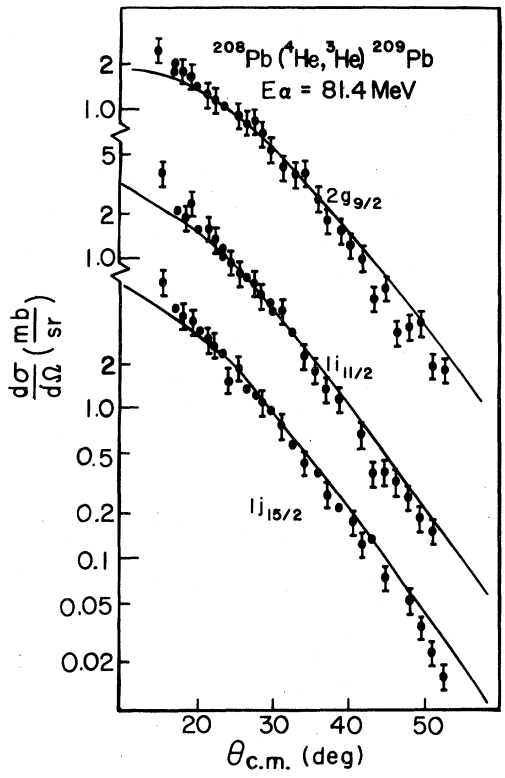

FIG. 7. (^{4}He,^{3}He) differential cross sections at 81.4 MeV (see caption of Fig. 2).

The spectroscopic factors obtained are quite similar to those of the (α,t) reactions, showing small, if any, energy dependence. In contrast to the $(\alpha,{}^3\mathrm{He})$ studies of Tickle and Gray[4] or previous (d,p) (Refs. 15,16) and (t,d) (Ref. 17) experiments, we find the $\frac{15}{2}^-$ state to be more pure single particle state than the $\frac{11}{2}^+$ state. To a large extent this result arises from the use of a smaller radius and diffuseness for the spin orbit component of the bound state potential, thereby leading to an effective spin-orbit strength less than that used in the previous analyses. The spin-orbit potential has a large effect on the calculated cross section for these high angular momentum states, as has been demonstrated in Ref. 4. An increase in the spin-orbit strength will lead to reasonable agreement with the other results, considering the uncertainties in extracted spectroscopic factors. However, we prefer to use the present bound state geometry to allow direct comparison with the heavy ion transfer reactions of Ref. 1.

V. CONCLUSIONS

We have made consistent alpha elastic scattering data measurements on ^{208}Pb at 40, 60, and 80 MeV, and have obtained potentials whose energy dependence is in good agreement with previous results.

We have also measured the (α,t) and $(\alpha,{}^3\mathrm{He})$ reactions on ^{208}Pb. Our finite range DWBA calculations reproduce the angular distributions relatively well particularly at the two higher energies. The spectroscopic factors obtained generally change by less than 15% in doubling the bombarding energy.

Our results verify that the spectroscopic factor for transferring either a proton or neutron onto the ground state of ^{208}Pb with a projectile in the 10–20 MeV/nucleon range, is approximately unity and has no energy dependence. This automatically leads to the conclusion that the strong energy dependence observed in the $(^{16}\mathrm{O},{}^{15}\mathrm{N})$ reaction cannot be attributed to any property associated with the states in ^{209}Bi. This discrepancy clearly arises from the use of heavy ion projectiles. Unfortunately, our present results do not indicate whether the problem with the heavy ion analysis arises from polarization effects, coupled-channel effects, or improper optical potentials as suggested in Ref. 2. However, these data provide additional tests of reaction theories including such effects. Clearly, any effects improving the heavy ion spectroscopic factor results must leave the (α,t) analysis unaffected.

ACKNOWLEDGMENTS

This work was supported in part by the U.S. National Science Foundation. The authors would like to thank the staff of the cyclotron for their service and dedication during these experimental runs. We also thank C. Samanta for her assistance in the experimental runs and with data analysis. The authors would also like to thank the University of Maryland Computer Science Center for their generous allocation of computer time for the DWBA calculations.

*Present address: Lawrence Berkeley Laboratory, Berkeley, California.

[1]C. Olmer *et al.*, Phys. Rev. Lett. 38, 476 (1977); Steven C. Pieper *et al.*, Phys. Rev. C 18, 180 (1978); C. Olmer *et al.*, ibid. 18, 205 (1978).

[2]S. Khanna and Steven C. Pieper (private communication).

[3]J.S. Lilley and Nelson Stein, Phys. Rev. Lett. 19, 709 (1967).

[4]Robert Tickle and W.S. Gray, Nucl. Phys. A247, 187 (1975).

[5]P.P. Singh, P. Schwandt, and G.C. Yang, Phys. Lett. 59B, 113 (1975); G.C. Yang, PhD. thesis, Indiana University, 1975 (unpublished).

[6]A. Nadasen *et al.*, Phys. Rev. C 18, 2792 (1978).

[7]N.S. Chant and J.N. Craig, Phys. Rev. C 14, 1763 (1976).

[8]N. Frascaria, J.P. Didelez, N.S. Chant, and C.C. Chang, Phys. Rev. C 16, 603 (1977).

[9]E. Friedman, A. Moalem, D. Suraqui, and S. Mordechai, Phys. Rev. C 15, 1604 (1977).

[10]F.D. Becchetti, Jr. and G.W. Greenless, in *Proceedings of the Third International Symposium on Polarization Phenomena in Nuclear Reactions, Madison, Wisconsin, 1970,* edited by H.H. Barschall and W. Haeberli (University of Wisconsin Press, Madison, 1971), p. 682.

[11]A. Djaloeis, J.P. Didelez, A. Galonsky, and W. Oelert,

Annual Report of Kernforschungsanlage Jülich, 1977, p. 2.
[12]M. Hyatkutake *et al.*, Nucl. Phys. A311, 161 (1978).
[13]W.C. Parkinson *et al.*, Phys. Rev. 178, 1976 (1969).
[14]E.R. Flynn, R.A. Hardekopf, J.D. Sherman, J.W. Sunier, and J.P. Coffin, Nucl. Phys. A279, 394 (1977).
[15]C. Ellegaard, J. Kantele, and P. Vedelsby, Nucl. Phys. A129, 113 (1969).
[16]D.G. Kovar, N. Stein, and C.K. Bockelman, Nucl. Phys. A231, 266 (1974).
[17]G.J. Igo, P.D. Barnes, E.R. Flynn, and D.D. Armstrong, Phys. Rev. 177, 1831 (1969).